IX CONGRESSO BRASILEIRO DE
ENGENHARIA E CIÊNCIAS TÉRMICAS
9th BRAZILIAN CONGRESS OF THERMAL
ENGINEERING AND SCIENCES

Paper CIT02-0194

FRONT TRACKING IN RECIRCULATING FLOWS: COMPARISON BETWEEN TVD AND RCM METHODS IN SOLVING THE VOF EQUATION

Luiz F. Lopes Silva
fernando@peq.coppe.ufrj.br

Carlos E. Fontes
carlos@peq.coppe.ufrj.br

Paulo L. C. Lage
paulo@peq.coppe.ufrj.br
Programa de Engenharia Química, COPPE/UFRJ
CP 68502 – CEP 21945-970 – Rio de Janeiro, RJ, Brazil

Abstract. *One of the most challenging problems in several industries is the correct simulation of mold filling. The modeling and simulation of mold filling must include a method to capture the interface formed between the inlet fluid and the fluid that was initially in the mold. A commonly used front-capturing method in an Eulerian mesh is the volume-of-fluid (VOF) method. Due to the hyperbolic nature of VOF advection equation, its solution usually suffers from numerical diffusion and/or dispersion and high-order numerical schemes have to be employed in the discretization of the convective terms, such as the TVD (Total Variation Diminishing) schemes with dimensional splitting. The present contribution explores the usage of RCM (Random Choice Method) for the solution of the VOF color-function equation during mold filling with recirculating flows. It was shown that it is able to generate a solution without numerical diffusion of the front position. The Navier-Stokes equations in rectangular cavities have been solved by a finite-volume method using the SIMPLER algorithm, without considering surface tension effects at the interface. Filling simulations using the TVD and RCM methods are compared. The RCM was able to generate diffusion-free results, sharply defining the interface, even when topological changes (generation of droplets) occur due to the recirculating flow. However, due to its statistical characteristic, front behavior may vary between different simulation runs for the same problem, leading to an uncertainty in front position. This was numerically shown to be equivalent to a numerical diffusion for a 1-D problem.*

Keywords*: Interface capturing, Mold filling, RCM, TVD schemes, VOF schemes, Computational fluid dynamics.*

1. INTRODUCTION

Several different industrial processes include a filling step of some kind of cavity (thermoplastic injection molding, reaction injection molding, casting of metal pieces, food extrusion processes,...). The design of these cavities involves a very expensive trial and error procedure in order to avoid filling problems, like heterogeneity in the final piece or air entrapment. This is specially true in the polymer industry. Due to this fact, during the last two decades many researchers have been developing computational methods that allows the simulation of cavity filling what shortens the expensive empirical stage. One of the most challenging problem in constructing a successful simulator is to capture and track the interface formed between the inlet fluid and the fluid that was initially inside the cavity.

One way of capturing the moving interface between two immiscible fluids is to solve the fluid flow equations for both fluids on the same Eulerian mesh. The two fluids are modeled as a single continuum with property jumps at the interface. The interface propagation is then obtained through the solution of a transient scalar advection equation in the Eulerian mesh. Such solution is prone to suffer from numerical diffusion and dispersion problems, which are inherent to the numerical solution of hyperbolic equations by any discretization scheme when there exist discontinuities in the solution. A fluid-fluid interface is a contact discontinuity, and its resolution demands additional care. In this paper, two numerical solutions to this problem are presented and compared: the usage of a high order TVD-scheme developed by Chakravarthy and Osher (1984) and the usage of a RCM-scheme (Random Choice Method) adapted from Toro (1999). Both schemes use dimensional splitting.

TVD methods are one of the most significant achievements in the development of numerical methods for partial differential equations in the last 20 years or so, althouth the premilinary ideas can be traced as far back as 1959, with the pioneering work of Godunov and continued later by van Leer. In 1965, Glimm introduced the RCM and Colella (1982) contributed to develop and increase the knownledge of the method, considering its advantages and limitations.

In this work, the TVD and RCM performances for cavity filling simulation were compared for both non-recirculating and recirculating flows. In the filling, it was assumed that both fluids had the same properties. Thus, the

pressure and velocity fields could be firstly obtained for the steady-state flow throughout any cavity and then used to the filling simulation using both methods. This eliminates any flow field disturbance that would rise in a filling simulation for unsteady fluid flow. These steady-state flow solutions were obtained by solving the transient mass and momentum conservation equations using a finite-volume method and the SIMPLER algorithm until the steady-state flow was reached to a given tolerance. The surface tension effects at the interface were not included in the analysis.

2. FLUID DYNAMICS EQUATIONS

The 2D-cartesian mass and momentum conservation equations for a Newtonian fluid, with constant density and viscosity, used in the flow simulation through 2D-cavities are presented below in a dimensionless form.

$$\frac{\partial(\varphi)}{\partial\tau} + \mathrm{Re}_{ref}\cdot\frac{\partial(\varphi U)}{\partial X} + \mathrm{Re}_{ref}\cdot\frac{\partial(\varphi V)}{\partial Y} = 0 \tag{1}$$

$$\frac{\partial(\varphi U)}{\partial\tau} + \mathrm{Re}_{ref}\cdot\frac{\partial(\varphi UU)}{\partial X} + \mathrm{Re}_{ref}\cdot\frac{\partial(\varphi VU)}{\partial Y} = -\mathrm{Re}_{ref}\cdot\frac{\partial P}{\partial X} - \left[\frac{\partial T_{xx}}{\partial X} + \frac{\partial T_{yx}}{\partial Y}\right] \tag{2}$$

$$\frac{\partial(\varphi V)}{\partial\tau} + \mathrm{Re}_{ref}\cdot\frac{\partial(\varphi UV)}{\partial X} + \mathrm{Re}_{ref}\cdot\frac{\partial(\varphi VV)}{\partial Y} = -\mathrm{Re}_{ref}\cdot\frac{\partial P}{\partial Y} - \left[\frac{\partial T_{xy}}{\partial X} + \frac{\partial T_{yy}}{\partial Y}\right] \tag{3}$$

$$T_{xx} = -2\Gamma\cdot\frac{\partial U}{\partial X} + \frac{2}{3}\cdot\Gamma\cdot\left[\frac{\partial U}{\partial X} + \frac{\partial V}{\partial Y}\right] \tag{4}$$

$$T_{yx} = T_{xy} = -\Gamma\cdot\left[\frac{\partial U}{\partial Y} + \frac{\partial V}{\partial X}\right] \tag{5}$$

$$T_{yy} = -2\cdot\Gamma\cdot\frac{\partial V}{\partial Y} + \frac{2}{3}\cdot\Gamma\cdot\left[\frac{\partial U}{\partial X} + \frac{\partial V}{\partial Y}\right] \tag{6}$$

where

$$X = \frac{x}{D_{in}} \qquad Y = \frac{y}{D_{in}} \qquad U = \frac{u}{v_{med}} \qquad V = \frac{v}{v_{med}} \tag{7}$$

$$P = \frac{p - \rho g_y y - \rho g_x x}{\rho\cdot v_{med}^2} \qquad \tau = \frac{\mu_{ref}\cdot t}{\rho_{ref}\cdot D_{in}^2} \tag{8}$$

$$\mathrm{Re}_{ref} = \frac{D_{in}\cdot v_{med}\cdot\rho_{ref}}{\mu_{ref}} \qquad \Gamma = \frac{\mu}{\mu_{ref}} \qquad \varphi = \frac{\rho}{\rho_{ref}} \tag{9}$$

and t is the time, x and y are the spatial coordinates, ρ is the density, μ is the viscosity, ν is the kinematic viscosity, u is the velocity component in x direction, v is the velocity component in y direction, p is the pressure, g_i is the body force in i direction, D_{in} is the inlet width and v_{med} is the mean inlet velocity. The subscript ref refers to the inlet fluid properties.

After applying a finite-volume discretization on a staggered grid using the power-law scheme, the steady-state solution has been achieved using the SIMPLER scheme (Patankar, 1980). The numerical code has been tested against benchmark results for the backward facing step flow (Gartling, 1990) with good agreement (Fontes et al., 1999).

The numerical results were integrated using a mixed (relative and absolute) tolerance of 10^{-6} for the velocity components and 10^{-5} for the pressure values. A mixed tolerance smaller than 10^{-4} for all the variables in every control volume between two consecutive times was the criterion used to assume that the steady state was achieved.

3. VOF-TVD SCHEME

The Volume-of-Fluid (VOF) method is a interface capturing method (Hirt and Nichols, 1981; Ferziger and Pèric, 1997). The fluids on both sides of the interface are marked by either massless particles or an indicator (color) function. In the VOF method the advection of the color function F, given by Equation (10) in dimensionless form, has to be solved. The F field values are stored at in the staggered finite-volume grid similarly to the pressure field.

$$\frac{\partial F}{\partial \tau} + Re \cdot U \cdot \frac{\partial F}{\partial X} + Re \cdot V \cdot \frac{\partial F}{\partial Y} = 0 \tag{10}$$

As commented above, U and V are known form the steady-sate solution. The simulated physical situation corresponds to the steady flow of a fluid through the cavity that suddenly becomes colored and starts to displace the non-colored one. Obviously, if the physical properties remains the same, so do the velocity and the pressure fields. For a given volume, F is equal to 0 when the volume has no colored fluid, but it is equal to 1 when the volume is completely filled with the colored fluid. The interface has F-values between 0 and 1.

Typical problems associated to the solutions of hyperbolic equations like Equation (10) (numerical diffusion and dispersion) are reduced by the use of a Total Variation Diminishing (TVD) scheme. A good summary of TVD schemes is given by Sweby (1984) and Toro (1999). A numerical method is TVD if Equation (11) is valid for scalar conservation laws, where ξ is the transported variable and TV(ξ) is its total variation.

$$TV\left(\xi^{n+1}\right) \le TV\left(\xi^{n}\right), \quad \text{where} \qquad TV(\xi) = \sum_{i} \left|\xi_i - \xi_{i-1}\right| \tag{11}$$

Chakravarthy and Osher (1984) described one-dimensional second and third-order accurate TVD schemes with low truncation error. These schemes were used to solve advective equations, like Equation (10). Goodman and LeVeque (1985) have proved that there is no multidimensional TVD scheme, but Chakravarthy and Osher (1984) have shown that numerical results achieved using their scheme are extremely good. Based on its simplicity and good results, the Chakravarthy and Osher (1984) third-order scheme has been used in the present work. In order to try to keep the TVD characteristics of the 1-D scheme, a dimensional splitting was applied during the numerical solution of Equation (10). Therefore, the explicit discretized form of Equation (10), with dimensional splitting, is given by Equations (12) and (13), where $\Delta\tau^{1/2} = \Delta\tau/2$. The splitting algorithm, in accordance to Toro (1999), is described below.

(i) For each time step $\Delta\tau$, integrate first in X direction up to $\Delta\tau^{1/2}$ using Equation (12).
(ii) Then, using $F^{1/2}$, integrate in the Y direction up to $\Delta\tau$ by Equation (12), determining F.
(iii) In order to achieve second order accuracy for every-other time step, invert the X and Y integrations in the next time step $\Delta\tau$.

$$F_P^{1/2} = F_P^o - Re \cdot \Delta\tau^{1/2} \cdot \frac{U_P \cdot \left(F_e^o - F_w^o\right)}{\Delta X} \tag{12}$$

$$F_P = F_{AUX} - Re \cdot \Delta\tau^{1/2} \cdot \frac{V_P \cdot \left(F_n^{1/2} - F_s^{1/2}\right)}{\Delta Y} \tag{13}$$

The F-fluxes at the faces of the volumes are determined using the upwind-TVD scheme. For example, for east face, for each j line, the flux is given by Eqs. (14) to (21). In these equations the index P means position (i, j), E position $(i+1, j)$, e position $(i+1/2, j)$, ee position $(i+3/2, j)$, w position. When γ equals 1/3 and β equals 4 these equations correspond to a third-order upwind scheme. Equation (14) represents the flux given for the Engquist-Osher first-order scheme (Osher and Chakravarthy, 1984). The minmod function is defined by Equation (19) and it is used to define the limited fluxes given in Equations (17) and (18). The fluxes for the other faces are obtained by obvious changes of subscripts.

$$U_P F_e = U_i F_{i+\frac{1}{2}} = f_e + h_e \tag{14}$$

$$f_e = f_{i+\frac{1}{2}} = \max[0, U_i] \cdot F_i - \max[0, -U_i] \cdot F_{i+1} \tag{15}$$

$$h_e = \frac{1}{4}\left[\left(\overline{d\phi}_e^{+} + \overline{\overline{d\phi}}_w^{+}\right) + \gamma\left(\overline{d\phi}_e^{+} - \overline{\overline{d\phi}}_w^{+}\right)\right] - \frac{1}{4}\left[\left(\overline{\overline{d\phi}}_e^{-} + \overline{d\phi}_{ee}^{-}\right) + \gamma\left(\overline{\overline{d\phi}}_e^{-} - \overline{d\phi}_{ee}^{-}\right)\right] \tag{16}$$

$$\overline{d\phi}_e^{+} = \text{minmod}(d\phi_e^{+}, \beta d\phi_w^{+}), \quad \overline{\overline{d\phi}}_w^{+} = \text{minmod}(d\phi_w^{+}, \beta d\phi_e^{+}) \tag{17}$$

$$\overline{\overline{d\phi}}_e^{-} = \text{minmod}(d\phi_e^{-}, \beta d\phi_{ee}^{-}), \quad \overline{d\phi}_{ee}^{-} = \text{minmod}(d\phi_{ee}^{-}, \beta d\phi_e^{-}) \tag{18}$$

$$\text{minmod}(a,b) = \text{sign}(a)\cdot \max\left\{0, \min\left[|a|, b\,\text{sign}(a)\right]\right\} \tag{19}$$

$$d\phi_e^{+} = d\phi_{i+\frac{1}{2}}^{+} = U_i \cdot (F_{i+1} - F_i), \qquad U_i > 0 \tag{20}$$

$$d\phi_e^{-} = d\phi_{i+\frac{1}{2}}^{-} = U_i \cdot (F_{i+1} - F_i), \qquad U_i \le 0 \tag{21}$$

Osher and Chakravarthy (1984) prove that their scheme is stable only for Courant number, given by Equation (22) for both X and Y directions, equal or less than 0.4.

$$C_X = \frac{u\cdot\Delta t}{\Delta x} = Re\cdot\frac{U\cdot\Delta\tau}{\Delta X} \quad \text{and} \quad C_Y = \frac{v\cdot\Delta t}{\Delta y} = Re\cdot\frac{V\cdot\Delta\tau}{\Delta Y} \tag{22}$$

Boundary conditions for this equation are obvious: the cells outside the mold inlet are considered to be completely filled with color fluid (F = 1), all cells outside the mold at the outlet are considered to be completely filled with colorless fluid (F = 0) and there is no F flux at the other boundaries. In the beginning of the filling process, the mold is filled with colorless fluid (F = 0).

4. VOF-RCM SCHEME

Glimm (1965) introduced the Random Choice Method but it was Colella (1982) who really developed this numerical method, discussing its advantages and limitations. Essentially, the RCM is applicable to scalar problems in any number of dimensions without loosing its capability of keeping the perfect resolution of contact discontinuities, with no diffusion or dispersion. As F, in Equation (10) is a scalar variable, RCM perfectly matches the necessities of the VOF method. Silva and Lage (2001) show a 1-D successful application of this scheme.

RCM chooses randomly among possible solutions of local Riemann problems, associated to the dimensional splitting of Equation (10). The method used in this work is one given by Toro (1999) for a staggered grid in which a local 1-D Riemann problem is solved twice for each direction at each integration step: once between τ^n and $\tau^{n+1/2}$ and once between $\tau^{n+1/2}$ and τ^{n+1}. It is exactly because RCM solves the local Riemann problem that it does not present numerical diffusion. RCM stability is also dependent on the local Courant number, given by Equation (22). For the RCM used in this work, both Courant numbers have to be equal or less than 1.

The Riemann local problem for Equation (10) uses the local states (F_L and F_R) around the interface between two control volume. The exact solution of the 1-D local Riemann problem is shown in Fig.(1-a). It consists in a single contact discontinuity propagation from the origin with velocity u and inclination $\lambda = 1/u$. Naturally, the solution values are equal to F_L on the left of the straight line with inclination $\lambda = 1/u$ and equal to F_R on the right of it.

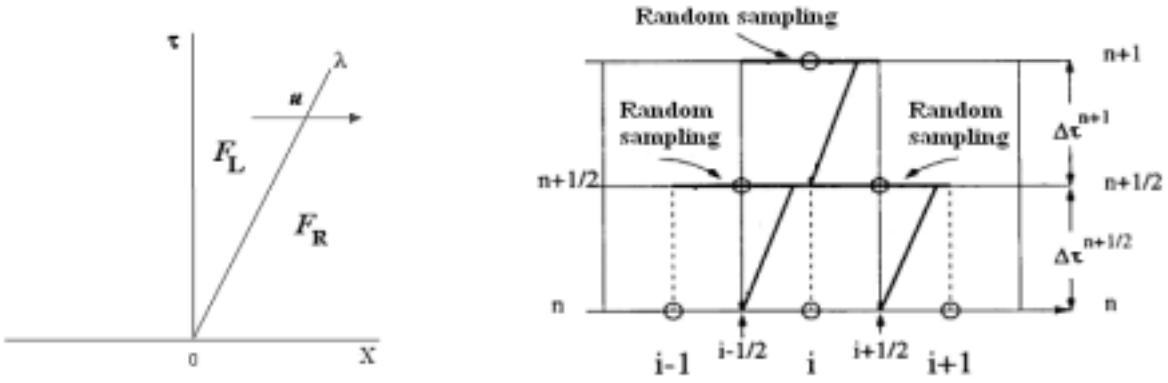

(a) (b)

Fig. 1: (a) The local 1-D Riemann problem; (b) Riemann problem applied to volume i.

In order to explain this method, lets consider its application to the integration of the F value in a given 1-D volume i of a uniform mesh in the X direction, as illustrated in Fig.(1-b), for a time step $\Delta\tau$. First the local 1-D Riemann problems are solved at both volume interfaces in the first half time step, $\Delta\tau_n^{1/2} = \Delta\tau_n/2$. At interface $(i-1/2)$, the discontinuity propagates a distance $d = X_{i-1/2} + C_{X,i+1/2}\cdot\Delta X/2$ during $\Delta\tau_n^{1/2}$. The position $r = X_{i-1/2} + \theta^n\cdot\Delta X$ is sampled by a random number $\theta^n \in [0,1]$. If $r \le d$ then $F_{i-1/2}^{n+1/2} = F_{i-1}^n$, otherwise $F_{i-1/2}^{n+1/2} = F_i^n$. A similar procedure is applied to the right interface using the same random number θ^n to obtain $\hat{F}_{i+1/2}^{n+1/2}$. Then, another random number is generated,

θ^{n+1}, and a similar procedure is applied to obtain the solution at the volume i itself at the end of the time interval, F_i^{n+1}. Thus, two new random numbers are generated for each time step and for each direction. The complete algorithm is described in the following.

(i) Solve the Riemann problems $RP\left(F_{i-1}^n, F_i^n\right)$ and $RP\left(F_i^n, F_{i+1}^n\right)$ to find the solutions $\hat{F}_{i-1/2}^{n+1/2}$ and $\hat{F}_{i+1/2}^{n+1/2}$;

(ii) For the first half time step $\Delta\tau_n^{1/2}$, random sample these solutions based on random number θ^n: $F_{i-1/2}^{n+1/2} = \hat{F}_{i-1/2}^{n+1/2}\left(\theta^n\right)$ and $F_{i+1/2}^{n+1/2} = \hat{F}_{i+1/2}^{n+1/2}\left(\theta^n\right)$;

(iii) Solve the Riemann problem $RP\left(F_{i-1/2}^{n+1/2}, F_{i+1/2}^{n+1/2}\right)$ to find the solution $\hat{F}_i^{n+1}$;

(iv) For the second half time step $\Delta\tau_n^{1/2}$, random sample this solution based on a new random number θ^{n+1}: $F_i^{n+1} = \hat{F}_i^{n+1}\left(\theta^n\right)$.

The same dimensional splitting applied to the VOF-TVD scheme is applied for the VOF-RCM scheme which uses twice the 1-D scheme just described. As RCM is intrinsically a statistical scheme, front behavior may vary between simulations runs for the same problem, what introduces some uncertainty about the actual position of the fluid interface. Due to this statistical nature, this uncertainty in the fluid interface decreases as the grid is refined. This occurs because more random numbers are generate to obtain the solution at a given time due to Courant number limitations. The random number generator used was the IMSL DRNUN subroutine that uses the generalized feedback shift register (GFSR) method.

5. UNIDIMENSIONALS TESTS

In order to verify the TVD and RCM implementations, a one dimensional test which tracks the movement of a square pulse was used. The simulations were carried out in an uniform grid, using TVD in Fig.(2) and RCM in Fig.(3). Wave positions and shapes are verified after 1.5 s, 3.5 s and 8 s. The agreement with the analytical solution is remarkable if the stability range of Courant number is respected.

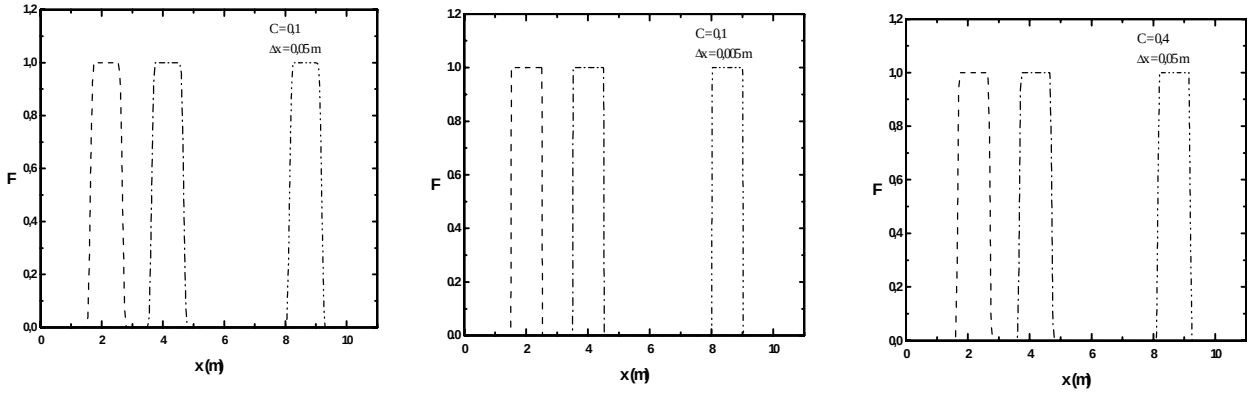

(a) (b) (c)

Fig. 2: Square pulse propagation in an uniform grid with constant velocity u = 0.1 m/s for different grids and Cournat numbers. The three profiles have exact positions at *x* =1.5, 3.5 and 8.0 m.

Fig. (2-a) shows that the use of coarse grids originates some numerical diffusion in the TVD solution. It was verified that a pulse propagation with a coarse grid deteriorates as the Courant decreases. When the grid is refined for the same Courant number (Fig. 2-b) or the Courant number is increased for the same grid (Fig. 2-c), this numerical diffusion vanishes.

Fig. (3) shows that all RCM results perfectly resolves the contact discontinuity of the interface. However, comparing Figs. (3-a) and (3-b) it is clear that some inaccuracy exists in the propagated pulse position for coarse grids. This results from errors in the pulse propagation velocity from the random character of the method. For the finer grid (Fig. 3-b), these errors basically disappear because of the large increase in the quantity of random numbers used to obtain the solution due to the Courant number limitation.

These errors in the position of the contact discontinuities are equivalent to numerical diffusion. This can be seen from Fig. (3-c) that shows the mean results of one hundred simulations of the pulse tracking in the coarse grid with different seeds in the random number generator. The behavior of the shape of the propagated pulse is similar to that is usually achieve in a single simulation when a diffusive scheme is used. In other words, the uncertainty in the positions of the discontinuities is numerically equivalent to the numerical diffusion of a low-order scheme.

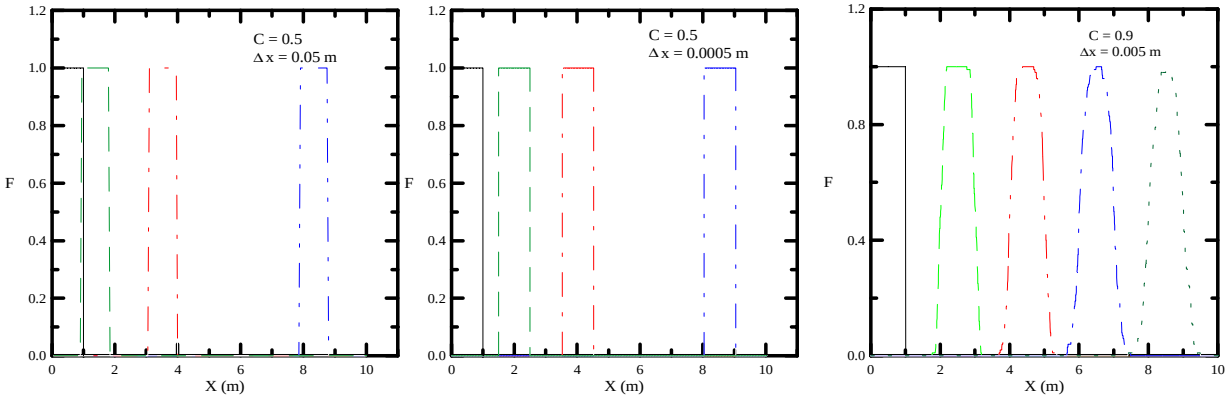

Fig. 3: Square pulse propagation in an uniform grid with constant velocity u = 0.1 m/s: (a) and (b) show the results for one simulation where the exact positions of the beginning of the propagated pulses are *x* =1.5, 3.5 and 8.0 m; (c) shows the mean of 100 simulation results where the exact positions of the beginning of the propagated pulses are *x* = 2, 4, 6 and 8.0 m.

6. TWO-DIMENSIONAL SIMULATION OF CAVITY FILLING

In order to compare the performance of the TVD and RCM methods associated to VOF scheme without any perturbation in the flow field, we decided to study the cavity filling using the steady-state flow solution. Two 2-D cavities are used, as shown in Fig.(4-a) and (4-b). Dimensions of the used mold cavity were LY = 20 cm and LX = 30.3 cm. The dimensions of the Backward Facing Step (BFS) cavity were 0.1 m × 3.0 m.

In a cavity like Fig. (4-a), called from now on mold cavity, a non-recirculating flow with low Reynolds number $\mathrm{Re} = 0.16$ was analyzed. The entry and exit widths of the mold are $D_{in} = D_{out} = 0.1 \cdot LX$. Velocity profile at the entry is parabolic with mean velocity equal to 0.031 m/s ($v_{med} = 0{,}031\,\mathrm{m/s}$) and the same velocity profile is applied to the exit. Other walls are considered impenetrable and non-slip conditions are imposed near to all walls. The flow in the BFS cavity, Fig (4-b), with $\mathrm{Re} = 400$, presents the typical recirculating flow with two opposing vortices. Velocity profile at the inlet is also parabolic, but the mean velocity is equal to 1 m/s. Due to the dimensions of this cavity ($LY = 30 \cdot LX$) it is possible to apply continuity conditions for the velocities and the pressure at its outlet (Gartling, 1990). The inlet width is $D_{in} = 0.5 \cdot LX$ and the width of the exit is LX itself. Impenetrable walls and non-slip conditions are also imposed to the others walls of this cavity. Simulations take place using a 200 × 200 grid for the mold cavity, and a 200 × 500 grid for the BFS cavity. A time step of 10^{-3} s was adequate for all TVD simulations and the BFS-RCM simulations. However, the mold-RCM simulations needed a larger time step (10^{-1}s) due to a loss of accuracy of the RCM for low Courant numbers that is explained in the next section (see the remarks concerning Fig. 9).

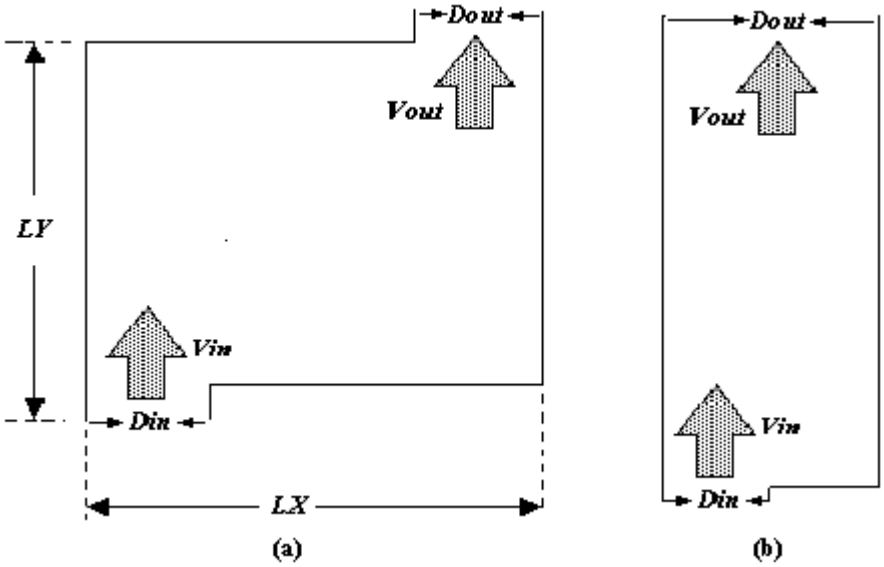

Fig.4 – Two-dimensional cavities: (a) rectangular mold. (b) backward facing step.

As mentioned in Section 2, a power-law scheme is used. The grid Peclet number is defined by Equation (23), where ζ is the grid length in the considered direction (X or Y).

$$Pe = Re_{ref} \cdot \frac{\Delta\zeta \cdot \varphi \cdot V}{\Gamma} \tag{23}$$

It is well known that power-law schemes allow numeric diffusion when the grid Peclet number exceeds 10 and the flow is oblique in relation to the grid (Patankar, 1980). In fact, in the BFS simulations, between the recirculating zones, there are very high Peclet numbers as 50 or 60. However, this phenomena do not invalidate this work conclusions because this paper goal is to compare two surface tracking methods under the same fluidynamic conditions. Furthermore, as commented in Section 2, velocity and pressure profiles have been successfully tested against Gartling's benchmark.

7. SIMULATION RESULTS

Fig. (5) and (6) compare the results achieved with the VOF-TVD scheme and the VOF-RCM scheme, respectively, for the non-recirculating flow inside the mold cavity. The filling patterns are very similar, but a remarkable difference has to be pointed out: as the filling continues the TVD scheme looses the interface sharpness due to a growing diffusion effect, while the RCM scheme does not show any diffusion. It can be noticed that the TVD solution shows the interface deeper inside the cavity than the RCM solution, although the same amount of fluid has entered the mold in both cases. Observing the behavior of the solutions near the bottom wall, it becomes clear that this difference may be explained by the diffusive characteristic of the two-dimensional "TVD" scheme, which pushes the incoming fluid towards the top wall, letting the other fluid remain in the region close to the bottom wall. Due to its statistical characteristic, RCM shows an interface with small fluctuations, which tend to disappears as the filling continues.

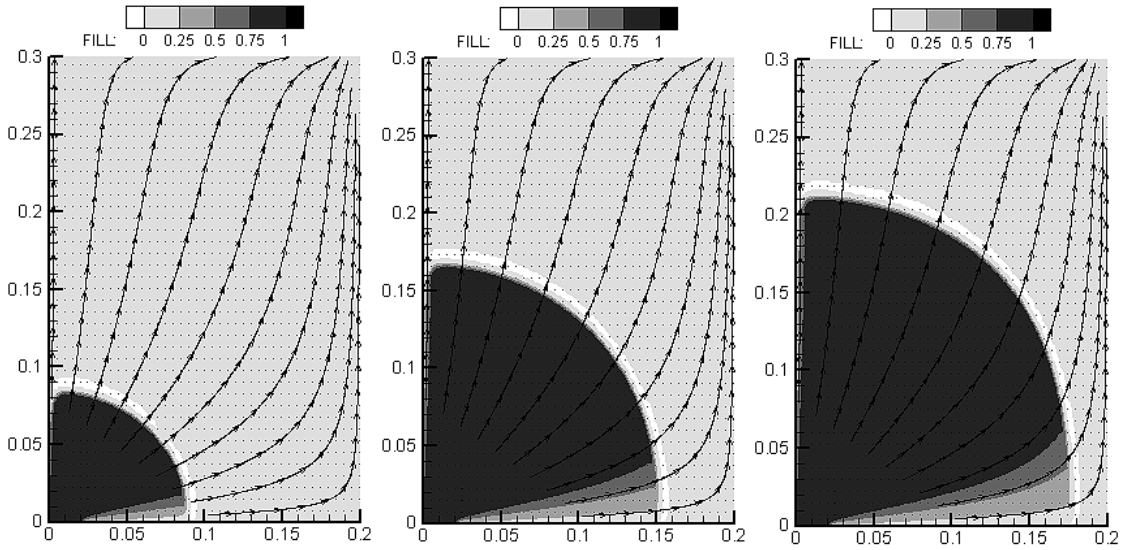

Fig.5 – Mold filling using VOF-TVD scheme with LX = 0.2 m ($\Delta x = 10^{-3}$ m): (a) after 10 s; (b) 40 s; (c) 70 s.

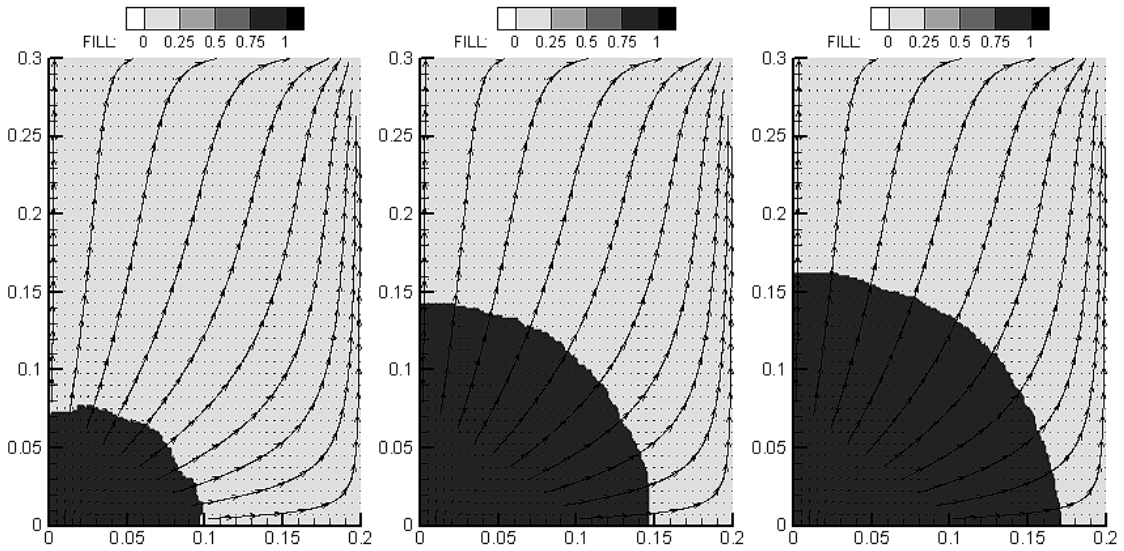

Fig.6 – Mold filling using VOF-RCM scheme with LX = 0.2 m ($\Delta x = 10^{-3}$ m): (a) after 10 s; (b) 40 s; (c) 70 s.

Fig. (7) and (8) show the simulation results in the BFS cavity. It is important to notice that the VOF-RCM and VOF-TVD methods show very similar results for the filling of this cavity. However, specifically at the vortex regions, the VOF-RCM method is capable of describing the droplets that are pulled away from the colored fluid by the rotating colorless fluid. The VOF-TVD scheme was incapable of describing this process. Furthermore, it suffers from intense numerical diffusion in these regions, what can be seen in Figs. (7-b), (7-c) and (7-d).

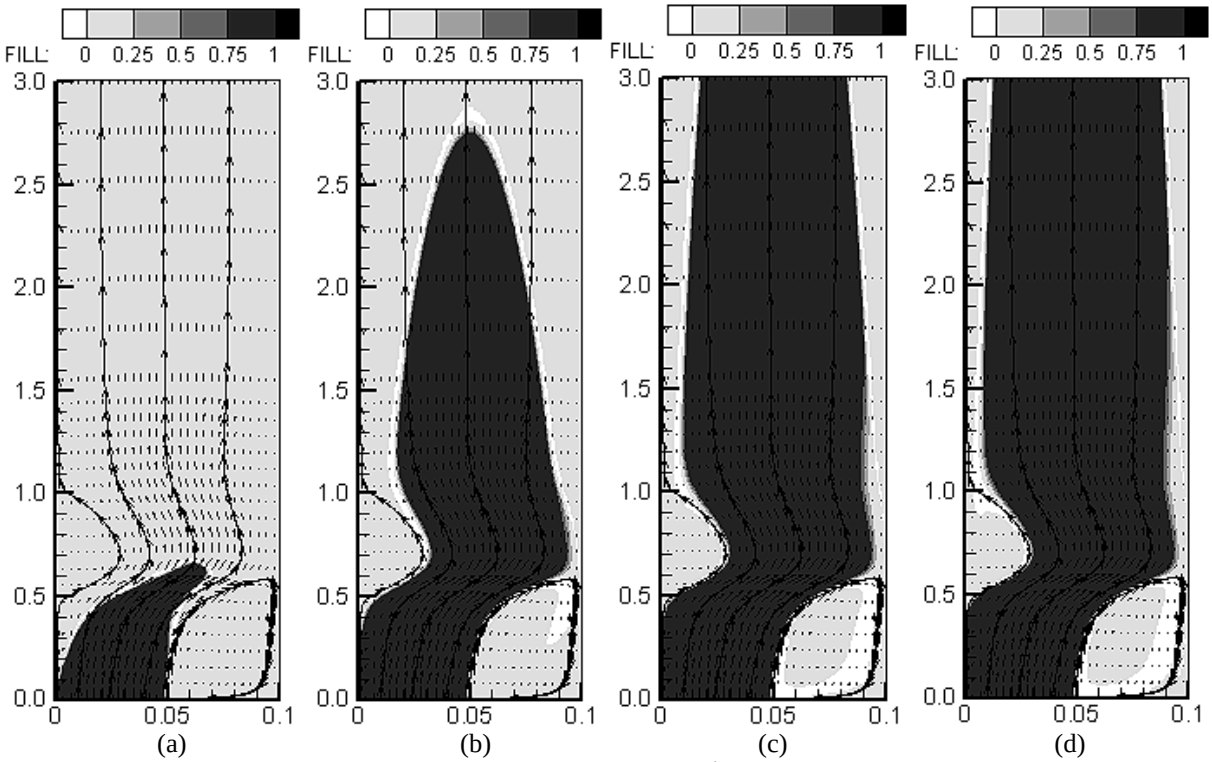

Fig.7 – BFS Cavity filling using VOF-TVD scheme ($\Delta x = 5.10^{-4}$ m): (a) after 0.5 s; (b) 3.5 s; (c) 6.5 s; (d) 9.5 s.

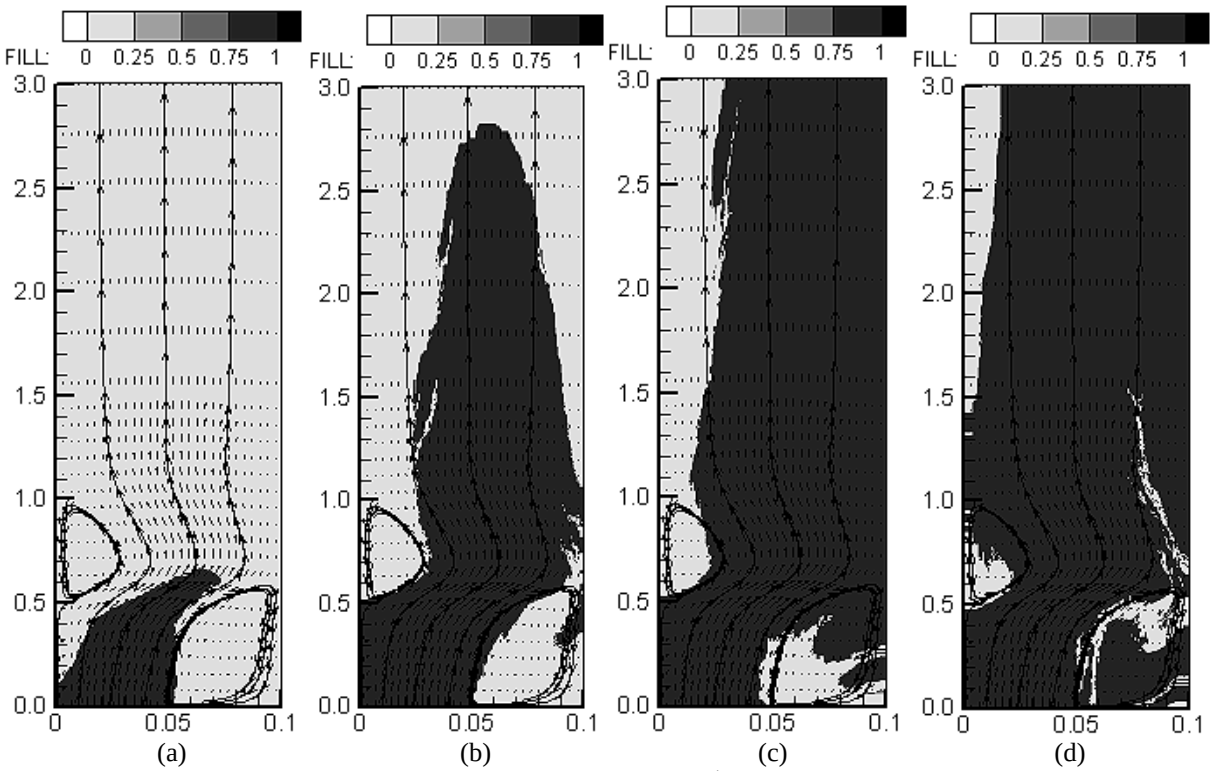

Fig.8 – BFS Cavity filling using VOF-RCM scheme ($\Delta x = 5.10^{-4}$ m): (a) after 0.5 s; (b) 3.5 s; (c) 6.5 s; (d) 9.5 s.

It is important to point out that Courant number restrictions remain in these two-dimensional simulations. As a matter of fact, Fig. (9-b) shows that the VOF-RCM scheme is unable to track the interface when Courant numbers were

less than $1 \cdot 10^{-3}$. It produces unrealistic results. On the other hand, VOF-TVD scheme (Fig. 9-a) does not show the same problem and tracks perfectly the interface.

It is important to enhance that all the simulations described above show an error in mass conservation less than 5%, except for the simulations using VOF-RCM scheme shown in Fig. (9-b).

Although the VOF-RCM scheme resolves perfectly the interface, it must be pointed out that with different seeds in the random number generator, different simulated results were obtained, even though their overall filling patterns are similar to each other. Thus, both VOF-TVD and VOF-RCM schemes seem to be adequate to describe the overall picture of the filling pattern in the mold and the BFS cavities.

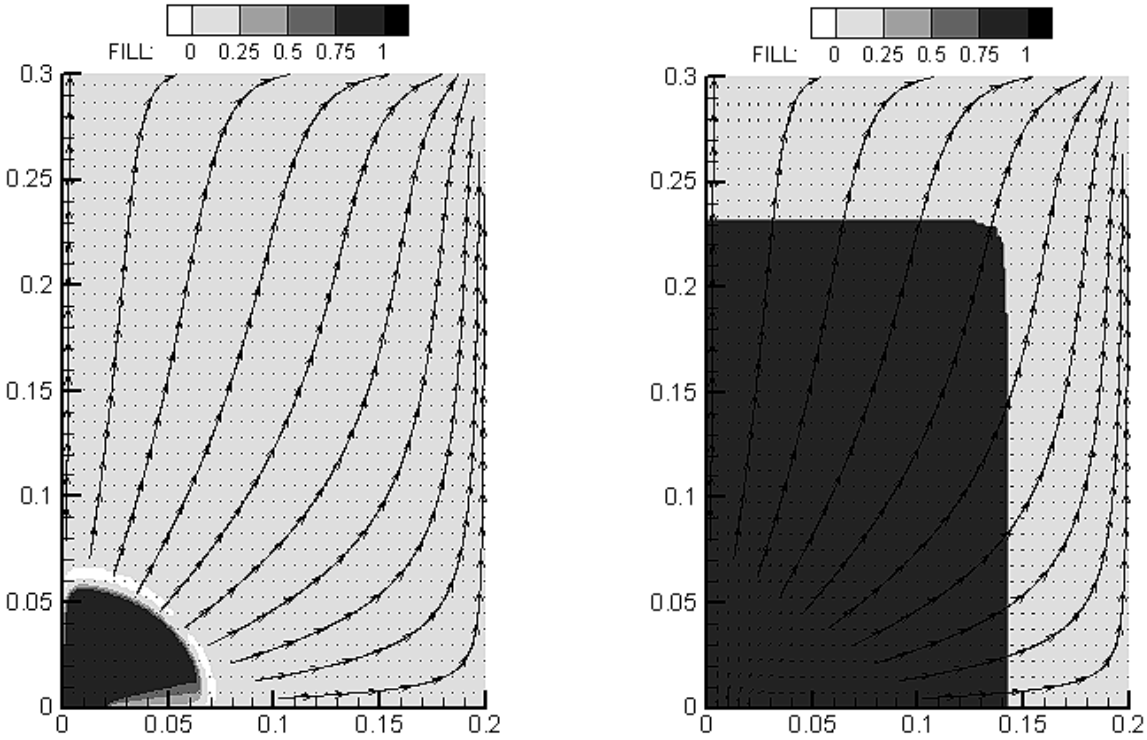

(a) (b)

Fig.9 – Low Courant number mold filling: comparison between VOF-TVD (a) and VOF-RCM (b) performances.

8. CONCLUSIONS

It was shown that the VOF-RCM scheme is able to generate diffusion-free results, sharply defining the interface, even when topological changes (droplet generation) occur due to the presence of intense recirculating flow. However, the statistical nature of RCM demands fine grids in order to simulate correctly the interface position. On the other hand, the VOF-TVD scheme suffers from some numerical diffusion but is less sensitive to low Courant numbers than the VOF-RCM scheme. It is important to realize that the front positions indicated by RCM method may vary between different simulations due its statistical nature. It was shown that these uncertainties are equivalent to numerical diffusion.

9. ACKNOWLEDGEMENTS

The authors acknowledge the financial support obtained from CNPq, grant number 520660/98-6.

10. REFERENCES

Chakravarthy, S.R. and Osher,S., 1984, A New Class of High Accuracy TVD Schemes for Hyperbolic Conservation Laws, AIAA paper 85-0363

Colella, P., 1982, Glimm's Method for Gas Dynamics, SIAM J. Sci. Stat. Comput., vol.3, n.1, pp.76-110.

Ferziger, J.H and Peric, M., 1997, Computational Methods for Fluid Dynamics, Springer, New York

Fontes, C.E., Lage, P.L.C., Pinto, J.C., 1999, Filling of Rectangular Molds Using the VOF Method and a TVD Discretization, Proceedings of the XV Brazilian Congress of Mechanical Engineering (Cobem), Águas de Lindóia, São Paulo, Brazil.

Gartling, D.K., 1990, A Test Problem for Outflow Boundary Conditions - Flow over a Backward Facing Step, International Journal for Numerical Methods in Fluids, vol.11, pp 953-967.

Glimm, J., 1965, Solution in the Large for Nonlinear Hyperbolic Systems of Equations. Comm. Pure. Appl. Math., v.18, pp.697-715.

Goodman, J.B. LeVeque, R.J., 1985, On the Accuracy of Stable Schemes for 2-D scalar Conservation Laws, Math. Comp., v. 45, p.15

Hirt, C.W., Nichols, B.D., 1981, "Volume of Fluid (VOF) Method for yhe Dynamics of Free Boundaries", Journal of Coputational Physics, v.39, pp. 201-225.

Osher, S., Chakravarthy, S., 1984, Very High Order Accurate TVD Schemes, ICASE Report no. 84-44, ICASE – NASA Langley Research Center, Hampton, Virginia.

Patankar, S.V., 1980, Numerical Heat Transfer and Fluid Flow, McGraw-Hill, New York.

Silva, L.F.L.R. & Lage, P.L.C., 2001, Método de Escolha Aleatória em Malhas Não Uniformes: Solução da Equação da Advecção Unidimensional, 4º Congresso Brasileiro de Engenharia Química em Iniciação Científica - COBEC-IC, Maringá - PR (in press).

Sweby, P.K., 1984, High Resolution Schemes Using flux Limiters for Hyperbolic Conservation Laws, SIAM Journal of Numerical Analysis, vol.21, n.5, pp. 995-1011

Toro, E. F., 1999, Riemann Solvers and Numerical Methods for Fluid Dynamics - A Pratical Introduction, 2nd Edition, Springer.